J|A|C|S
ARTICLES

Published on Web 07/09/2009

Antiplatelet and Thermally Responsive Poly(*N*-isopropylacrylamide) Surface with Nanoscale Topography

Li Chen,[†,§] Mingjie Liu,[‡,§] Hao Bai,[‡,§] Peipei Chen,[‡,§] Fan Xia,[†,§] Dong Han,[*,‡] and Lei Jiang[*,†]

Beijing National Laboratory for Molecular Sciences (BNLMS), Center for Molecular Sciences, Institute of Chemistry, Chinese Academy of Sciences, Beijing 100190, P. R. China, National Centre for NanoScience and Technology, Beijing 100190, P. R. China, and Graduate University of Chinese Academy of Sciences, Beijing 100049, P. R. China

Received March 14, 2009; E-mail: dhan@nanoctr.cn; jianglei@iccas.ac.cn

Abstract: Nanoscale topography was constructed on a thermally responsive poly(*N*-isopropylacrylamide) (PNIPAAm) surface by grafting the polymer from silicon nanowire arrays via surface-initiated atom transfer radical polymerization. The as-prepared surface showed largely reduced platelet adhesion in vitro both below and above the lower critical solution temperature (LCST) of PNIPAAm (~32 °C), while a smooth PNIPAAm surface exhibited antiadhesion to platelets only below the LCST. Contact angle and adhesive force measurements on oil droplets (1,2-dichloroethane) in water demonstrated that the nanoscale topography kept a relatively high ratio of water content on the as-prepared surface and played a key role in largely reducing the adhesion of platelets; however, this effect did not exist on the smooth PNIPAAm surface. The results can be used to extend the applications of PNIPAAm in the fields of biomaterials and biomedicine under human physiological temperature and provide a new strategy for fabricating other blood-compatible materials.

Introduction

Designing blood-compatible materials and devices is vital for implantation and many other medical uses. It is generally believed that when they are in contact with blood, most implanted material surfaces adsorb blood proteins, after which platelet activation and adhesion occur, causing blood coagulation and thrombosis.[1] Surface composition, charge, flexibility and wettability, etc. have an important influence on the blood compatibility of materials.[2,3] Among all these factors, wettability is one of the most important parameters affecting protein adsorption, platelet adhesion/activation, and blood coagulation.[4−6] Thus, controlling and adjusting the surface wettability is crucial to blood compatibility of biomaterials. To date, thermally responsive poly(*N*-isopropylacrylamide) (PNIPAAm) has attracted extensive attention because of its reversible conversion between hydrophilicity and hydrophobicity below and above its lower critical solution temperature (LCST, ~32 °C)[7] and its novel property of controlling the adhesion of cells as well as platelets.[8−10] Numerous works have been done to study and improve the surface properties of PNIPAAm.[11−13] However, few studies have truly noticed the influence of the nanoscale topography of the PNIPAAm surface on cells.[14,15] In fact, surface topography, especially nanoscale topography, elicits diverse cell behaviors, including changes in cell adhesion, cell orientation, cell motility, surface antigen display, etc.[16−19]

In this work, we successfully constructed a nanoscale topography on a PNIPAAm surface by introducing silicon nanowire arrays (SiNWAs), and investigated the interaction

[†] Institute of Chemistry, Chinese Academy of Sciences.
[‡] National Centre for NanoScience and Technology.
[§] Graduate University of Chinese Academy of Sciences.

(1) Hoffman, R.; Benz, E. J.; Shattil; S. J.; Furie, B.; Cohen, H. J. *Hematology: Basic Principles and Practice*; Churchill Livingstone: New York, 1991.
(2) *Blood-Surface Interactions: Biological Principles Underlying Haemocompatibility with Artificial Materials*; Cazenave, J. P., Davies, J. A., Kazatchkine, M. D.; van Aken, W. G., Eds.; Elsevier: Amsterdam, 1986.
(3) Lee, J. H.; Lee, H. B. *J. Biomed. Mater. Res.* **1998**, *41*, 304–311.
(4) Sethuraman, A.; Han, M.; Kane, R. S.; Belfort, G. *Langmuir* **2004**, *20*, 7779–7788.
(5) Xu, L. C.; Siedlecki, C. A. *Biomaterials* **2007**, *28*, 3273–3283.
(6) Faucheux, N.; Schweiss, R.; Lutzow, K.; Werner, C.; Groth, T. *Biomaterials* **2004**, *25*, 2721–2730.
(7) Gil, E. S.; Hudson, S. A. *Prog. Polym. Sci.* **2004**, *29*, 1173–1222.
(8) Okano, T.; Kikuchi, A.; Sakurai, Y.; Takei, Y.; Ogata, N. *J. Controlled Release* **1995**, *36*, 125–133.
(9) Takei, Y. G.; Aoki, T.; Sanui, K.; Ogata, N.; Sakurai, Y.; Okano, T. *Biomaterials* **1995**, *16*, 667–673.
(10) Uchida, K.; Sakai, K.; Ito, E.; Kwon, O. H.; Kikuchi, A.; Yamato, M.; Okano, T. *Biomaterials* **2000**, *21*, 923–929.
(11) Matsuda, N.; Shimizu, T.; Yamato, M.; Okano, T. *Adv. Mater.* **2007**, *19*, 3089–3099.
(12) Xu, F. J.; Zhong, S. P.; Yung, L. Y. L.; Kang, E. T.; Neoh, K. G. *Biomacromolecules* **2004**, *5*, 2392–2403.
(13) Kikuchi, A.; Okano, T. *J. Controlled Release* **2005**, *101*, 69–84.
(14) Kwon, O. H.; Kikuchi, A.; Yamato, M.; Sakurai, Y.; Okano, T. *J. Biomed. Mater. Res.* **2000**, *50*, 82–89.
(15) Xu, F. J.; Zhong, S. P.; Yung, L. Y. L.; Tong, Y. W.; Kang, E. T.; Neoh, K. G. *Biomaterials* **2006**, *27*, 1236–1245.
(16) Stevens, M. M.; George, J. H. *Science* **2005**, *310*, 1135–1138.
(17) Flemming, R. G.; Murphy, C. J.; Abrams, G. A.; Goodman, S. L.; Nealey, P. F. *Biomaterials* **1999**, *20*, 573–588.
(18) Curtis, A.; Wilkinson, C. *Biomaterials* **1997**, *18*, 1573–1583.
(19) Sun, T. L.; Tan, H.; Han, D.; Fu, Q.; Jiang, L. *Small* **2005**, *1*, 959–963.

between this surface and platelets in vitro. The as-prepared surface (SiNWA−PNIPAAm) showed largely reduced platelet adhesion both below and above the PNIPAAm LCST, while the smooth PNIPAAm surface exhibited antiadhesion to platelets only below the LCST. It was demonstrated that the nanoscale topography kept a relatively high ratio of water content on the SiNWA−PNIPAAm surface and played a key role in largely reducing the adhesion of platelets; however, this effect did not exist on the smooth PNIPAAm surface.

PNIPAAm is a well-known thermally responsive polymer that shows an extended hydrophilic chain conformation below its LCST in aqueous solution and undergoes a phase transition to insoluble and hydrophobic aggregates above the LCST.[20−22] Okano and co-workers have thoroughly investigated this transition of surface wettability, which affects the platelet contacting activation and adhesion.[8,9] Platelets can be activated and adhere to the PNIPAAm surface above its LCST, while below it, the platelets cannot adhere and tend to detach from the PNIPAAm surface.[10] Unfortunately, this would restrict the application of PNIPAAm and its copolymers in vivo as potential drug delivery systems,[23] since the effect may bring activation and adhesion of platelets and thus cause subsequent blood coagulation and thrombosis. Recently, SiNWAs have attracted extensive interest in many fields, such as nanodevices, photovoltaic cells, biosensors, etc.[24,25] Moreover, the surfaces of SiNWAs also show unique nanostructures in topography that are well-matched with the size of platelets (2−4 μm). In order to investigate the interaction between platelets and the nanoscale topography of a PNIPAAm surface, we combined the composition of PNIPAAm and the nanostructures of a SiNWA surface. In our experiment, the SiNWA was fabricated by a versatile, low-cost method through chemical etching of crystalline silicon in $AgNO_3$/HF aqueous solution.[26] PNIPAAm was then grafted onto SiNWA through surface-initiated atom transfer radical polymerization (SI-ATRP).[27,28] In vitro testing for platelet adhesion was conducted on SiNWA−PNIPAAm and control surfaces, and further characterizations via scanning electron microscopy (SEM), transmission electron microscopy (TEM), X-ray photoelectron spectroscopy (XPS), atomic force microscopy (AFM), and contact angle measurements were used to investigate the surface properties. Details concerning SiNWA preparation, the SI-ATRP process, and the platelet adhesion treatment are given in the Experimental Section.

Results and Discussion

Both SEM and TEM images show that the SiNWA−PNIPAAm surface possesses unique nanoscale topography. Figure 1a displays a top-view SEM image of the SiNWA. Many silicon nanoclusters, formed by several nanowires combined together,

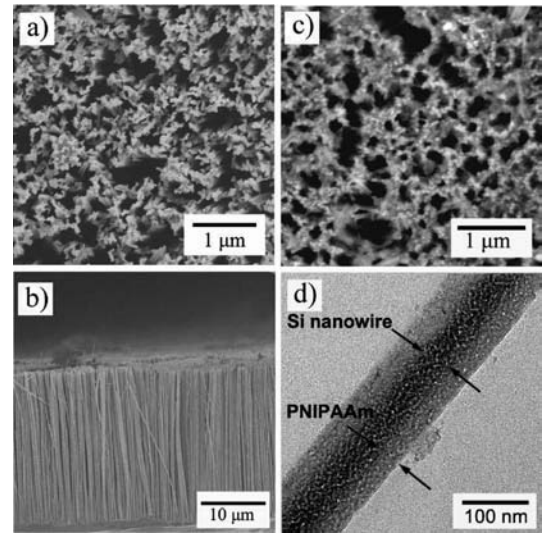

Figure 1. Morphologies of SiNWA and PNIPAAm-grafted SiNWA (SiNWA−PNIPAAm). (a) SEM top view of the as-prepared SiNWA. (b) Cross-sectional SEM view of an SiNWA with a length of 25 ± 3.3 μm. (c) SEM top view of SiNWA−PNIPAAm, where a thin layer of PNIPAAm was grafted onto the SiNWA surface while retaining the nanoscale topography. (d) TEM image of a single silicon nanowire enwrapped by PNIPAAm. The diameter of the single silicon nanowire is ∼64.2 nm, and the thickness of the PNIPAAm layer is ∼32.3 nm.

can be clearly observed on the surface. As evidenced by the cross-sectional SEM image (Figure 1b), most of the nanowires are perpendicular to the silicon wafer substrate and have uniform diameters in the range 50−100 nm (average value 69.7 ± 4.3 nm) and lengths of 25 ± 3.3 μm. Polymerization of *N*-isopropylacrylamide monomer by SI-ATRP using SiNWA produced a thin layer of PNIPAAm on the SiNWA surface (Figure 1c). The TEM image (Figure 1d) clearly shows a single silicon nanowire enwrapped by PNIPAAm, as the interface of these two components is evident. According to the TEM image, the diameter of the single silicon nanowire is ∼64.2 nm, and the thickness of the PNIPAAm layer is ∼32.3 nm. Further characterization of the SiNWA−PNIPAAm surface was conducted by XPS (Figure S1 in the Supporting Information). The XPS wide-scan spectrum of the surface shows that composition of surface elements is mainly C, N, and O (Figure S1a). The C 1s core-level spectrum of the surface (Figure S1b) can be curve-fitted for three peak components with binding energies of ∼284.8, 285.5, and 288.0 eV, attributable to the C−H, C−N, and N−C═O species, respectively.[12,29] The XPS results prove that the material surface is grafted with PNIPAAm, indicating an effective SI-ATRP procedure in our work.

Testing for platelet adhesion was carried out in vitro via the platelet-suspension method and assessed by environmental SEM (ESEM) imaging. Here, three kinds of control surfaces were introduced for comparison with the SiNWA−PNIPAAm surface: a pristine smooth silicon wafer (Si), a bare SiNWA, and a PNIPAAm-grafted smooth silicon wafer (Si−PNIPAAm). As shown in Figure 2a, the density of adhered platelets on the Si surface was (1.0 ± 0.2) × 10^6 platelets/cm^2 at 37 °C, which is a little higher than the value of (5.7 ± 1.6) × 10^5 platelets/cm^2 at ambient temperature (∼20 °C). The difference for the two temperature conditions is mainly due to the low activity of platelets below the physiological temperature of 37 °C. For the

(20) Schild, H. G. *Prog. Polym. Sci.* **1992**, *17*, 163–249.
(21) Heskins, M.; Guillet, J. E.; James, E. *J. Macromol. Sci., Chem.* **1968**, *A2*, 1441–1445.
(22) Jeong, B.; Kim, S. W.; Bae, Y. H. *Adv. Drug Delivery Rev.* **2002**, *54*, 37–51.
(23) Kavanagh, C. A.; Rochev, Y. A.; Gallagher, W. A.; Dawson, K. A.; Keenan, A. K. *Pharmacol. Ther.* **2004**, *102*, 1–15.
(24) Kim, W.; Ng, J. K.; Kunitake, M. E.; Conklin, B. R.; Yang, P. D. *J. Am. Chem. Soc.* **2007**, *129*, 7228–7229.
(25) Li, Y.; Qian, F.; Xiang, J.; Lieber, C. M. *Mater. Today* **2006**, *9*, 18–27.
(26) Peng, K. Q.; Yan, Y. J.; Gao, S. P.; Zhu, J. *Adv. Funct. Mater.* **2003**, *13*, 127–132.
(27) Huang, X. Y.; Wirth, M. J. *Anal. Chem.* **1997**, *69*, 4577–4580.
(28) Sun, T. L.; Wang, G. J.; Feng, L.; Liu, B. Q.; Ma, Y. M.; Jiang, L.; Zhu, D. B. *Angew. Chem., Int. Ed.* **2004**, *43*, 357–360.
(29) Beamson, G.; Briggs, D. *High-Resolution XPS of Organic Polymers: the Scienta ESCA300 Database*; Wiley: Chichester, U.K., 1992.

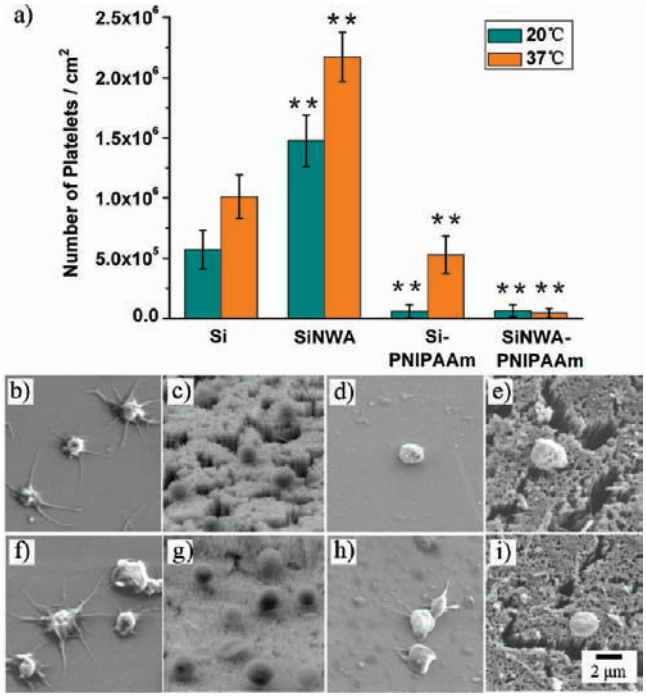

Figure 2. Number and morphology of adhered platelets. (a) Statistical histogram of the number of adhered platelets on different surfaces at 20 °C (blue bars) and 37 °C (orange bars): Si, pristine smooth silicon wafer; SiNWA, silicon nanowire array; Si−PNIPAAm, PNIPAAm grafted onto Si; SiNWA−PNIPAAm, PNIPAAm grafted onto SiNWA. The ** labels indicate significant differences ($p < 0.01$) in comparison with Si. The values are means of ten samples, and the error bars denote the standard deviation. (b−i) ESEM images of adhered platelets on (b, f) Si, (c, g) SiNWA, (d, h) Si−PNIPAAm, and (e, i) SiNWA−PNIPAAm at 20 and 37 °C, respectively.

SiNWA surface, the density of adhered platelets was the highest one among the four samples [$(2.2 \pm 0.2) \times 10^6$ platelets/cm^2 at 37 °C and $(1.5 \pm 0.2) \times 10^6$ platelets/cm^2 at 20 °C]. Subsequently, the Si−PNIPAAm surface showed significantly less platelet adhesion than the Si surfaces but remarkable temperature-responsive behavior [$(5.8 \pm 1.5) \times 10^5$ platelets/cm^2 at 37 °C, 1 order of magnitude higher than the value of $(6.0 \pm 6.7) \times 10^4$ platelets/cm^2 at 20 °C]. Surprisingly, only a few platelets were found to adhere on the SiNWA−PNIPAAm surface at both 20 and 37 °C, which means that the temperature-responsive behavior was eliminated in this manner.

Additionally, morphological changes in platelets adhered on different surfaces were certainly observed in our work. Figure 2b−i displays the detailed morphology of adhered platelets on different surfaces at 20 and 37 °C by ESEM imaging. On the Si surface (Figure 2b,f), the platelets were highly activated and fully spread out with many typical pseudopods at both 20 and 37 °C. On the SiNWA surface, the adhered platelets were ball-shaped with less-spreading pseudopods (Figure 2c,g), probably because of the structural restriction on the platelets by the silicon nanowires. However, as shown in Figure 2d,h, the platelets exhibited different morphologies on the Si−PNIPAAm surface at 20 and 37 °C. The adhered platelets were spherical with obvious protuberances but few pseudopods at 20 °C, whereas at 37 °C, the platelets were spread out to some extent with a few pseudopods. This suggests that PNIPAAm inhibited platelet adhesion below its LCST and that this effect died out above its LCST, possibly as a result of reduced platelet−surface interactions caused by hydration of PNIPAAm chains as the temperature decreased.[10] In regard to the SiNWA−PNIPAAm surface (Figure 2e,i), it is very noticeable that adhered platelets were barely found on the surface at both 20 and 37 °C. The few platelets on the surface kept a disk shape free of pseudopods. This result indicates that the SiNWA−PNIPAAm surface could largely reduce the adhesion and activation of platelets.

To understand this result, it should be noted that although Si and SiNWA surfaces are hydrophilic, there is always a thin layer of SiO_2 at the silicon surface. Iler has shown that over the normal pH range the surface of SiO_2 is weakly negatively charged and that the charge density is virtually constant between pH 3 and 8.[30] Hence, the adhesion of platelets on the SiNWA surface may be complicated by the presence of surface charges at the SiO_2−water interface. The electrostatic attraction between this charged surface and protein molecules is often the driving force for adsorption from solution onto the solid surface and mostly causes irreversible adsorption of proteins on the charged surface.[31,32] Since attachment of cells/platelets is a secondary process that significantly depends on the nature of the adsorbed layer of protein,[33] the charged Si and SiNWA surfaces in our experiment can easily cause platelet adhesion and certainly have no antiplatelet effect.

To the best of our knowledge, the PNIPAAm surface is hydrophilic and antiadhesive to platelets below the LCST but hydrophobic and adhesive to platelets above the LCST.[10] The nanoscale topography was supposed to enlarge this thermally responsive change, rendering the surface more hydrophilic and antiadhesive below the LCST and more hydrophobic and adhesive above it.[28] However, it turned out that this nanofabricated PNIPAAm surface showed the antiadhesive property to platelets both below and above the LCST. Therefore, surface wettability, a most important parameter affecting platelet behavior, certainly should be considered. In previous work reported by Sun et al.,[19] a nanostructured superhydrophobic surface showed novel antiadhesive properties to platelets. However, in the work presented here, the antiadhesive nanostructured PNIPAAm surface shows thermally responsive switching between hydrophilic and hydrophobic states. In an air system, for the Si−PNIPAAm surface, the contact angle (CA) of a 3 μL water droplet increased from 70.1 ± 1.3° to 88.5 ± 4.5° (Figure 3a) when the temperature was switched from 20 to 37 °C, while for the SiNWA−PNIPAAm surface, the CA changed from 20.7 ± 3.1° to 106.4 ± 5.3° (Figure 3b). Accordingly, in a water system, for the same Si−PNIPAAm surface, the CA of a 3 μL oil droplet (1,2-dichloroethane) decreased evidently from 121.1 ± 5.2° to 103.7 ± 6.3° (Figure 3c), while for the same SiNWA−PNIPAAm surface, the CA stayed almost constant, and the surface remained in the superoleophobic state when the temperature was switched from 20 to 37 °C again (Figure 3d). This result is crucial for understanding the change in platelet adhesion on the Si−PNIPAAm and SiNWA−PNIPAAm surfaces at 20 and 37 °C. Because the platelet adhesion experiment was conducted in phosphate buffered saline (PBS, pH 7.4), the wettability of the PNIPAAm surface in the liquid phase should be taken into account. It has been reported by Liu et al.[34] that a hydrophilic

(30) Iler, R. K. *The Chemistry of Silica*; Wiley: New York, 1979.
(31) Nakanishi, K.; Sakiyama, T.; Imamura, K. *J. Biosci. Bioeng.* **2001**, *91*, 233–244.
(32) Su, T. J.; Lu, J. R.; Thomas, R. K.; Cui, Z. F.; Penfold, J. *J. Phys. Chem. B* **1998**, *102*, 8100–8108.
(33) Mrksich, M.; Whitesides, G. M. *Annu. Rev. Biophys. Biomol. Struct.* **1996**, *25*, 55–78.
(34) Liu, M. J.; Wang, S. T.; Wei, Z. X.; Song, Y. L.; Jiang, L. *Adv. Mater.* **2009**, *21*, 665–669.

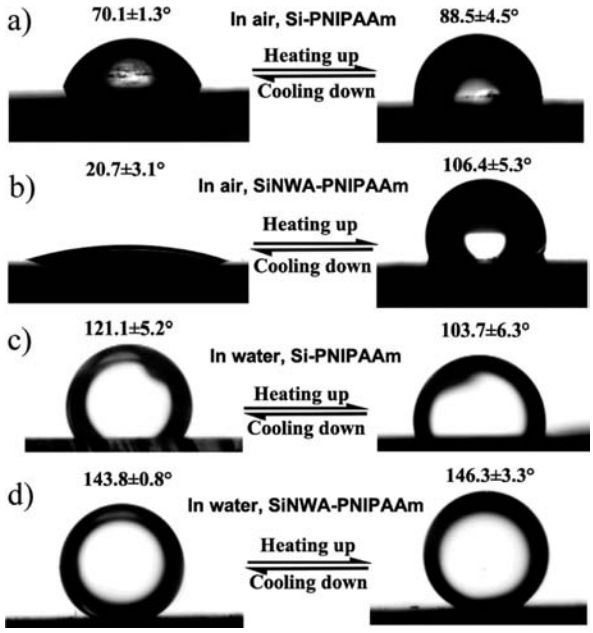

Figure 3. Contact angle images for Si−PNIPAAm and SiNWA−PNIPAAm surfaces under different conditions. The temperature was set to (left) 20 and (right) 37 °C. (a) CAs of water droplets on the Si−PNIPAAm surface in air, where the change in CA was ∼18.4°. (b) CAs of water droplets on the SiNWA−PNIPAAm surface in air, where the change in CA was ∼85.7°. (c) CAs of oil droplets (1,2-dichloroethane) on the Si−PNIPAAm surface in water, where the change in CA was ∼17.4°. (d) CAs of oil droplets on the SiNWA−PNIPAAm surface in water, where the surface remained a superoleophobic state.

surface in a water/air/solid system shows oleophobic behavior in an oil/water/solid system (see Scheme S1 and Note S1 in the Supporting Information). Moreover, a water-trapped composite rough surface, such as fish skin, can even exhibit a superoleophobic property due to its high water content. Therefore, the CA results for the water system offer a direct proof that the SiNWA−PNIPAAm surface was composed with relatively high ratio of water content, which leads to a nonresponsive superoleophobic state in comparison with the responsive oleophobic state of the Si−PNIPAAm surface in water. It is obvious that the nanoscale topography plays a key role in keeping water molecules on the SiNWA−PNIPAAm surface.

For the Si−PNIPAAm and SiNWA−PNIPAAm surfaces, the adhesive forces on oil droplets in water also varied remarkably. In our experiment, force changes were recorded by a high-sensitivity micromechanical balance system[35] when the Si−PNIPAAm and SiNWA−PNIPAAm surfaces were controlled to contact and leave a 1 μL oil droplet. The Si−PNIPAAm surface exhibited remarkable adhesion to the oil droplet, always drawing the droplet with great shape distortion and then causing it to break; this implies that the adhesive force should be larger than the stretch force (Figure 4a,b). The stretching force for this surface was 19.0 ± 2.4 μN at 37 °C and 14.5 ± 2.5 μN at 20 °C. However, for the SiNWA−PNIPAAm surface, the oil droplet could only be stretched to an elliptical shape, with almost no residuum on the surface (Figure 4c,d). The adhesive force here was only 3.2 ± 1.7 μN at 37 °C and 4.6 ± 1.8 μN at 20 °C, much smaller than that on Si−PNIPAAm surface. This result is in great consistence with the results of the CA measurements

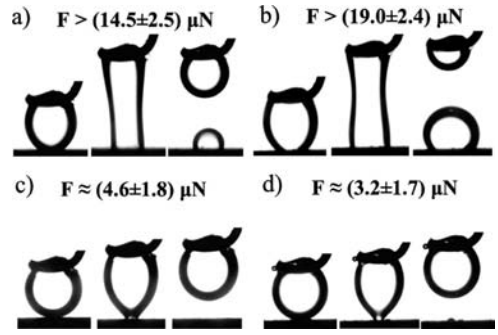

Figure 4. Adhesive force measurements on different substrates using oil droplets (1,2-dichloroethane) as detecting probes. Each measurement includes three steps: (left) the oil droplet contacts the surface; (middle) the oil droplet is leaving the surface; (right) the oil droplet has left the surface. (a) At 20 °C, the smooth Si−PNIPAAm surface shows a large adhesive force and a high amount of residuum. (b) At 37 °C, the smooth Si−PNIPAAm surface shows a large adhesive force and a higher amount of residuum. (c) At 20 °C, the SiNWA−PNIPAAm surface shows a low adhesive force and almost no residuum. (d) At 37 °C, the SiNWA−PNIPAAm surface shows a low adhesive force and almost no residuum.

in water, showing higher water content on the SiNWA−PNIPAAm surface than on the Si−PNIPAAm surface.

AFM was also used to characterize the smooth PNIPAAm surface to investigate its adhesion behavior to platelets at the micro/nano scale. As shown in Figure 5a−d, a 3 μm × 3 μm area of the Si−PNIPAAm surface was scanned (tapping mode) in situ using a Si_3N_4 tip in water at 20 and 37 °C (the green circles represent the same area). Increasing the temperature from 20 to 37 °C resulted in shrinkage of the nanopapillas on the PNIPAAm surface, as can be observed in the topography images in Figure 5a,b. Moreover, as a useful tool for characterization of the adhesion force between a tip and a sample,[36,37] topography and recognition (TREC) images (Figure 5c,d) were used to display different adhesive forces between the tip and surface at 20 and 37 °C. More dark regions can be observed in Figure 5d than in Figure 5c, and especially in the green-circle region, the color changes dramatically from light-yellow to black. These increasing dark regions represent stronger hydrophobic−hydrophobic interactions between the tip and the surface (the Si_3N_4 tip is hydrophobic) at 37 °C than at 20 °C, indicating a transition of the PNIPAAm surface from hydrophilic to hydrophobic state.[38] Direct quantitative measurement of the adhesion force between the Si_3N_4 tip (force constant = 0.121 N/m) and the PNIPAAm surface was also conducted in contact mode at 20 and 37 °C. As shown in Figure 5e, the typical force−distance curve displays a sharp peak in the adhesion force during separation of the tip and surface at 37 °C, while only an inapparent peak existed at 20 °C. The average adhesion force (based on 30 curves measured at each location and five locations at each temperature) was 0.50 nN at 20 °C and 1.18 nN at 37 °C, and the corresponding distributions of the observed adhesion forces are visualized in Figure 5f. The temperature-dependent switching of the adhesion force between the Si_3N_4 tip and the PNIPAAm surface can be ascribed to a hydrophobic attractive force, which gives clear evidence for the hydrophilic−hydrophobic phase transition of the PNIPAAm surface, leading to responsive adhesion of platelets from 20 to 37 °C.

(35) Jin, M. H.; Feng, X. J.; Feng, L.; Sun, T. L.; Zhai, J.; Li, T. J.; Jiang, L. *Adv. Mater.* **2005**, *17*, 1977–1981.
(36) Stroh, C.; Wang, H.; Bash, R.; Ashcroft, B.; Nelson, J.; Gruber, H.; Lohr, D.; Lindsay, S. M.; Hinterdorfer, P. *Proc. Natl. Acad. Sci. U.S.A.* **2004**, *101*, 12503–12507.
(37) Ge, G. L.; Han, D.; Lin, D. Y.; Chu, W. G.; Sun, Y. X.; Jiang, L.; Ma, W. Y.; Wang, C. *Ultramicroscopy* **2007**, *107*, 299–307.
(38) Jones, D. M.; Smith, J. R.; Huck, W. T. S.; Alexander, C. *Adv. Mater.* **2002**, *14*, 1130–1134.

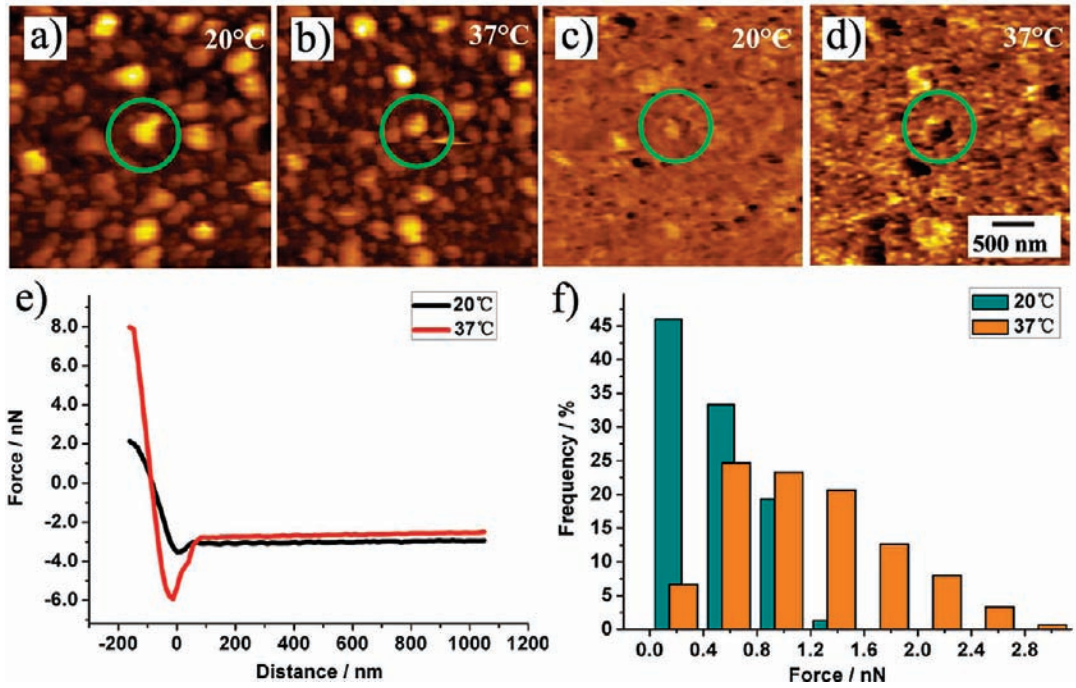

Figure 5. AFM mapping of the PNIPAAm surface and direct measurement of the adhesion force between the tip and sample. (a−d) In situ AFM images of the PNIPAAm surface (green circles represent the same area; scale bar 500 nm): (a, b) topography images at 20 and 37 °C, respectively (*Z* range 700 nm), showing the shrinkage of the nanopapilla on the PNIPAAm surface with increasing temperature; (c, d) TREC images at 20 and 37 °C, respectively (*Z* range 2.5 V), in which the change in color from light-yellow to black indicates the surface transition from the hydrophilic state to the hydrophobic state. (e) Typical temperature-dependent switching of the adhesion force between a Si_3N_4 probe tip and the PNIPAAm surface. The adhesion force was ∼0.50 nN at 20 °C (black line) and 1.18 nN at 37 °C (red line). (f) Histograms of the adhesion forces between the probe tip and the PNIPAAm surface at 20 °C (blue bars) and 37 °C (orange bars).

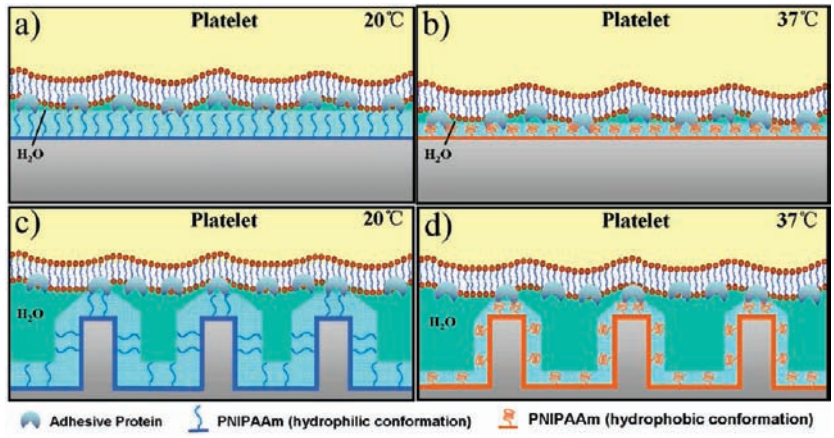

Figure 6. Hypothetical platelet adhesion mechanisms for different surfaces. (a) On the Si−PNIPAAm surface at 20 °C, extended polymer chains form a hydration layer that prevents adhesive proteins of platelets from adsorbing. (b) On the Si−PNIPAAm surface at 37 °C, the polymer chains crouch to a hydrophobic state, enabling adhesive proteins to adsorb. (c) On the SiNWA−PNIPAAm surface at 20 °C, water is trapped into the interstices of the nanowire arrays, causing a higher hydration ratio of the surface and lower protein adhesion. (d) On the SiNWA−PNIPAAm surface at 37 °C, the water-trapping effect changes the surface wettability from a hydrophobic state to a hydrophilic state, thus largely reducing the adsorption of adhesive proteins.

To the best of our knowledge, it is more difficult for protein or cells to adsorb on a hydrophilic polymer surface [e.g., poly(ethylene glycol) or poly(ethylene oxide)] than a hydrophobic polymer surface, mainly because of the high water content in the hydration layer of these polymer outer chains.[39−41] Meanwhile, the hydrophilic/hydrophobic transition of the PNIPAAm surface has been reported to be the main reason affecting the responsive adhesion of cells and platelets.[8,10] However, that mechanism may not suitable when nanoscale topography is considered. A new mechanism is proposed to explain why the SiNWA−PNIPAAm surface can largely reduce the adhesion of platelets relative to the Si−PNIPAAm surface, as shown in Figure 6a−d. In the present work, for the smooth Si−PNIPAAm surface, PNIPAAm chains form a hydration layer that prevents adhesive proteins of platelets from adsorbing at 20 °C (Figure 6a), while at 37 °C, the PNIPAAm chains crouch into a hydrophobic state, enabling adhesive proteins to adsorb (Figure 6b). However, for the SiNWA−PNIPAAm surface, water molecules are trapped in the interstices of the nanowire

(39) Prime, K. L.; Whitesides, G. M. *J. Am. Chem. Soc.* **1993**, *115*, 10714–10721.
(40) Chen, S. F.; Zheng, J.; Li, L. Y.; Jiang, S. Y. *J. Am. Chem. Soc.* **2005**, *127*, 14473–14478.
(41) Harder, P.; Grunze, M.; Dahint, R.; Whitesides, G. M.; Laibinis, P. E. *J. Phys. Chem. B* **1998**, *102*, 426–436.

arrays, causing a higher hydration ratio of the surface (Figure 6c). This effect was evidenced by the oil droplet CA and adhesive force measurements in water. Hence, the increased water content of the surface largely reduces the adsorption of adhesive proteins of platelets. Moreover, since the PNIPAAm surface is already hydrophilic at 20 °C but hydrophobic at 37 °C, this water-trapping effect brings a greater change in the wettability of PNIPAAm surface at 37 °C than at 20 °C (Figure 6d). This is why largely reduced adhesion of platelets could be achieved by the introduction of nanoscale topography at both 20 and 37 °C, i.e., both below and above the PNIPAAm LCST. Furthermore, the improved interfacial property of SiNWA−PNIPAAm inspires us to suggest that optimization of chemical characteristics in combination with micro/nanoscale topography could yield new functional materials.

Conclusion

In summary, SI-ATRP of PNIPAAm onto a silicon nanowire array yielded a surface showing typical nanoscale topography and significantly reduced activation and adhesion of platelets (relative to the Si, SiNWA, and Si−PNIPAAm surfaces) both below and above the PNIPAAm LCST. Both contact angle and adhesive force measurements in water revealed that the nanoscale topography kept a relatively high ratio of water content on the PNIPAAm surface, which played a key role in largely reducing the adhesion of platelets. We believe that the work presented here will extend the applications of PNIPAAm in the field of biomaterials and biomedicine at human physiological temperature and offer a new strategy for fabricating other blood-compatible materials.

Experimental Section

Fabrication of SiNWA. Silicon wafers were cut into rectangular strips, soaked in 3:1 H_2SO_4 (97%)/H_2O_2 (30%) for 30 min, and then thoroughly rinsed with deionized water. Cleaned silicon strips were put into the etching solution ([HF] = 5.0 mol L^{-1} and [$AgNO_3$] = 0.015 mol L^{-1}), sealed at 50 °C for 20 min, immersed in 20% nitric acid for 1 min, and finally rinsed with deionized water two or three times.

SI-ATRP of PNIPAAm onto SiNWA. The SiNWA strips were immersed in a saturated aqueous NaOH/ethanol solution for 5 min and subsequently in HNO_3 (0.1 M) for 10 min to generate surface hydroxyl groups. After they were washed with deionized water and dried using nitrogen gas, they were heated to reflux in toluene containing 5 wt % aminopropyltrimethoxysilane (ATMS) for 6 h, affording chemically bonded $-NH_2$ groups on the surface. The strips were rinsed with toluene and dichloromethane and then immersed in dry dichloromethane containing 2% (v/v) pyridine. The polymerization initiator bromoisobutyryl bromide was added dropwise into the solvent containing the strips at 0 °C; the system was left at 0 °C for 1 h and then at room temperature for 12 h, after which the strips were cleaned with dichloromethane and acetone. Polymerization of NIPAAm was achieved by immersing the strips with the initiator grafted onto the surface into a degassed solution of NIPAAm (0.8 g) in a 1:1 (v/v) mixture of H_2O and CH_3OH (5 mL) containing CuBr (0.032 g, 0.23 mmol) and pentamethyldiethylenetriamine (PMDETA; 0.14 mL) for 2 h at 60 °C. When the polymerization was over, the strips were rinsed with deionized water two or three times and then blown dry with a flow of nitrogen.

Preparation of Platelet Suspension. Blood was drawn from male rats (Wistar, 400 g) into a syringe containing a 3.8% sodium citrate solution [9:1 (v/v) blood/anticoagulant], in accordance with institutional policies. Next, platelet-rich plasma (PRP) was prepared by centrifugation (1100 rpm for 10 min). After ACD anticoagulant and EDTA were added, the PRP was centrifuged at 160*g* for 10 min twice to separate the platelets and platelet-poor plasma (PPP). The platelets were then suspended in PBS at a final concentration of $\sim 10^6$ cells/mL.

Platelet Adhesion and Treatment. Two groups of samples were placed in the platelet suspension and incubated for 1 h, one at room temperature (~20 °C) and the other at 37 °C. After incubation, the two groups of samples were rinsed with PBS at 20 and 37 °C, respectively, to remove loosely attached platelets, fixed with 3% glutaraldehyde in PBS for 30 min at the respective experimental temperatures, and then transferred to storage at 4 °C overnight. Finally, the samples were gradiently dehydrated by ethanol and treated by critical CO_2 drying for subsequent ESEM observation. The platelet adhesion on different surfaces was assessed by randomly selecting 10 images for each surface and then counting the number of platelets.

Acknowledgment. This work was supported by the National Research Fund for Fundamental Key Projects (2007CB936403, 2006CB705600, 2005CB724700) and the National Natural Science Foundation of China (20571077, 90709054). We thank Prof. Ruomei Qi, Dr. Haifeng Meng, Dr. Yanxia Zhang, and Dr. Fei Wang for helpful discussions and Mrs. Xie for technical support.

Supporting Information Available: XPS results, a scheme illustrating surface wetting behavior in air/water, theoretical analysis, and additional experimental details. This material is available free of charge via the Internet at http://pubs.acs.org.

JA9019935